Int. J. Solids Structures Vol. 23, No. 12, pp. 1601–1614, 1987
Printed in Great Britain.

0020-7683/87 $3.00+ .00

ANALYTICAL MODELING OF PRECURSOR DECAY IN STRAIN-RATE DEPENDENT MATERIALS

THEODORE NICHOLAS
Air Force Wright-Aeronautical Laboratories (MLLN), Wright-Patterson AFB, OH 45433, U.S.A.

and

A. M. RAJENDRAN and DAVID J. GROVE
University of Dayton Research Institute, Dayton, OH 45469, U.S.A.

Transmitted by J. D. Achenbach

(*Received* 8 *October* 1986; *in revised form* 10 *March* 1987)

Abstract—A finite difference computer code is used to numerically simulate uniaxial strain waves generated from plate impact experiments. The incremental flow law of Bodner and Partom is used to describe the strain rate dependent plastic flow in 7039 aluminum and C1008 steel. Constants determined from Hopkinson bar tests and plate impact experiments are found adequate to predict precursor decay in these materials. A mathematical definition of the Hugoniot elastic limit (HEL) based on a plastic strain offset criterion is proposed.

INTRODUCTION

The knowledge of the dynamic behavior of materials is important in understanding and analytically modeling impact phenomena. Computational approaches to complex dynamic phenomena such as rod–target interactions and the design of self-forging fragments through the use of sophisticated two- and three-dimensional finite difference computer codes have received increasing attention in the past decade. The significant advances in computer technology coupled with the increased complexity and cost of weapons system experiments have led to an increase in the use of analytical simulations for preliminary design and parametric studies of all types of ballistics problems. One of the key ingredients necessary to make these computations realistic is the accurate description of the constitutive behavior and failure characteristics of materials.

Modeling of material behavior is generally approached by treating the relationships between the spherical and deviatoric parts of stress and strain separately. Spherical or hydrostatic stresses and strains are linearly related through the bulk modulus for low pressures and through an equation of state or Hugoniot for high pressures. The Hugoniot provides a locus of thermodynamically admissible stress states during shock wave propagation. For the deviatoric part of the stresses and strains, a simple elastic–plastic material model combined with a yield criterion and plastic flow law are commonly used. These models, in general, assume that the plastic flow is independent of the hydrostatic stress for moderate pressure levels. An alternate approach to a yield criterion and flow law is the use of constitutive equations which decompose strain rates into elastic and plastic components, and in which the plastic strain rate is always non-zero and determined from an incremental flow law. This approach, first used by Bodner[1] for dynamic plasticity problems will be illustrated and used in this investigation.

The modeling of the dynamic plastic deformation of metals can be broken down into three basic categories. In the first, the plastic deformation is considered to be independent of rate of strain. In this case, quasi-static data are utilized and the constitutive equation does not involve time derivatives of strain. Computationally and experimentally, this is the simplest approach to dynamic plasticity. For many metals, however, the assumption of strain-rate independence is unrealistic, particularly at high strain rates[2]. The second approach to dynamic plasticity is the use of a rate-independent theory with a single dynamic stress–strain relation which is different than the quasi-static one. In this case, it is assumed

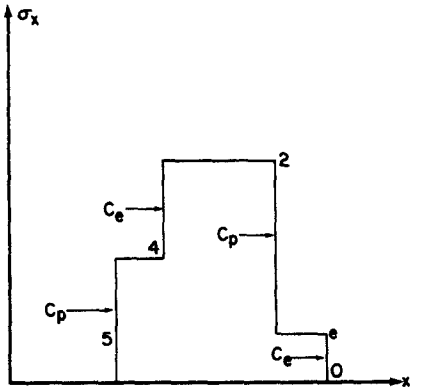

Fig. 1. Schematic of idealized stress profile in uniaxial strain wave propagation.

that all dynamic behavior is governed by a single dynamic relationship but that strain-rate effects do not have to be explicitly incorporated into the constitutive equations. As in the first case, the mathematics is relatively simple; however some type of dynamic test is required to obtain the dynamic relationship. This approach can work for certain problems where strain rates do not vary significantly and where the data for the stress–strain behavior were obtained at similar strain rates. The third approach to dynamic plasticity assumes that the material is strain-rate dependent. This requires both the assumption of the form of the rate-dependent constitutive law and experimental data covering a range of strain rates. Mathematically and experimentally, it is the most difficult approach, but probably the most realistic in terms of dynamic plastic deformation of metals.

To use this third approach, experimental data must be obtained which will allow the determination of constants in a proposed constitutive equation. The data can be obtained from constant-strain-rate tests at high rates using techniques such as the split Hopkinson bar, or from analysis of transient wave propagation phenomena[3]. Split Hopkinson bar tests and uniaxial stress wave experiments in long rods are generally limited to strain rates of approximately 10^3 and $10^2\,s^{-1}$, respectively. To achieve higher rates, waves of uniaxial strain as generated in plate impact experiments can be used. Specifically, the amplitude of the elastic precursor, the Hugoniot elastic limit (HEL), has been used as one measure of the dynamic yield strength of a material.

It is the purpose of this investigation to demonstrate the applicability of a rate-dependent constitutive model to shock wave propagation. The model, the constants of which are determined from high strain rate Hopkinson bar and steady state HEL data, is applied to the prediction of shock wave profiles in plate impact experiments. In particular, we examine some of the characteristics of the HEL and their relationship to the dynamic plastic behavior of materials. A numerical study using both rate-dependent and rate-independent constitutive relations is employed. A series of computer generated plots is presented to illustrate some of the characteristics of the HEL. In addition to proposing a mathematical definition of the HEL, observations on how experimental HEL data can be used in validating constitutive relations are given.

THE HUGONIOT ELASTIC LIMIT (HEL)

The HEL is defined as the amplitude of the elastic precursor in a uniaxial strain wave as generated in plate impact experiments. An idealized wave profile is shown schematically in Fig. 1. The elastic wave travels at a velocity C_e and has an amplitude $0e$, the HEL. A slower plastic wave travels at velocity C_p. For thin plate impacts, unloading elastic and plastic waves are also present.

Under uniaxial strain conditions, the relation between stress and strain in the direction of wave propagation depends on the dynamic plastic behavior and constitutive law. Generally speaking, there is an elastic region and a plastic region, as in uniaxial stress. For an elastic–perfectly plastic material, the stress–strain curves in uniaxial stress and uniaxial

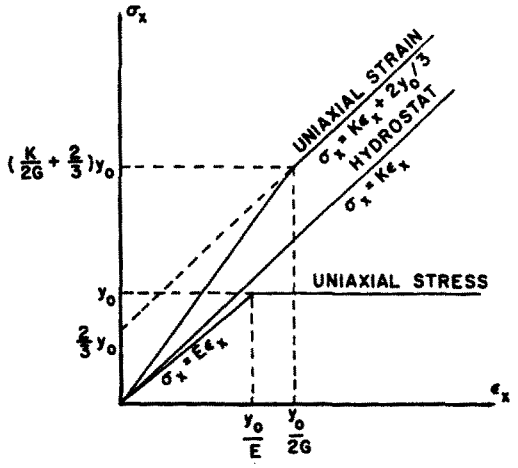

Fig. 2. Stress–strain behavior for elastic–perfectly plastic material.

strain are shown in Fig. 2. The elastic limit in uniaxial strain, σ_{HEL}, can be related to the yield stress in uniaxial stress, y_0, through

$$\sigma_{HEL} = \left(\frac{K}{2G} + \frac{2}{3}\right) y_0 \tag{1}$$

assuming a Von Mises or Tresca yield criterion. For a more general constitutive relationship or yield criterion, the definition of the HEL becomes less precise. Experimentally, the HEL is taken as the stress amplitude of the elastic precursor. This can be obtained directly from experimental measurements using an embedded stress gauge[4] or, more commonly, from rear surface velocity[5] measurements, through

$$\sigma_{HEL} = \tfrac{1}{2}\rho c \bar{v} \tag{2}$$

where $\bar{v}$ is the velocity corresponding to the peak amplitude of the elastic precursor ahead of the slower plastic wave, ρ the mass density, and c the elastic wave velocity given by

$$c = \sqrt{\left(\frac{K + \frac{4}{3}G}{\rho}\right)}. \tag{3}$$

The amplitude of $\bar{v}$ or σ_{HEL} is generally considered to be a constant after some distance of wave propagation from the impact plane. It is this "constant" value that is used in eqn (1) to determine the equivalent dynamic yield stress, y_0, in uniaxial stress. No specific strain rate is easily associated with this value as will be explained later.

For plate impact configurations where stresses can be measured close to the impact plane, the HEL has been observed to achieve values which are considerably higher than the steady state value. This is generally interpreted as evidence of the strain-rate dependence of the material. Numerous analyses have been conducted relating the transient amplitude of the HEL to plastic strain rate as derived by Duvall[6]

$$\frac{\partial \bar{\sigma}}{\partial t} = -G\dot{\varepsilon}^p \tag{4}$$

where $\bar{\sigma}$ is the HEL, G the shear modulus, and $\dot{\varepsilon}^p$ the plastic strain rate in the direction of propagation of the shock wave. Equation (4) is obtained from the one-dimensional equations of motion and continuity, and the characteristic equation along the leading elastic precursor. The validity of eqn (4) is limited to conditions of small strain and for plastic strain rates of the form

$$\dot{\varepsilon}^p = \dot{\varepsilon}^p(\sigma, \varepsilon^p). \tag{5}$$

Equation (4) has been used in conjunction with precursor decay observations to determine the relaxation function, $\dot{\varepsilon}^p$. Most of these computations have used forms for $\dot{\varepsilon}^p$ which have been derived from dislocation dynamics concepts, or, conversely, have attempted to establish or validate laws governing the number or velocity of dislocations as a function of stress and plastic strain. They have generally involved fitting experimental data solely of precursor amplitudes as a function of propagation distance or time. Few attempts have been made to relate precursor decay to constitutive models derived from high strain rate data from other sources. Jones *et al.*[7] used Hopkinson bar data and various *ad hoc* stress–strain rate models. The models attempted to simulate various forms of strain rate dependence while still matching high strain rate Hopkinson bar data obtained at one high strain rate. Various forms were used in eqn (4) and then integrated to predict precursor decay. In this manner, constants were obtained to fit both the precursor decay data and the Hopkinson bar results. These one-dimensional stress–strain rate models were empirical in nature and formulated mainly to fit the precursor decay data.

Few analyses have evaluated viscoplastic models which are used for plastic wave studies under uniaxial stress condition or for matching high strain rate data over a wide range of strain rates. Rajendran[8] and Swift and Fyfe[9] used the exponential form of the viscoplastic model of Perzyna[10] to describe precursor decay phenomena. The method of characteristics approach was used in these works to calculate precursor decay along the leading elastic shock front.

Note that in the application of eqn (4) no formal definition of the HEL is required. No attempt was made in these investigations to compare the constitutive models to other types of data. There have been no finite difference analyses, to our knowledge, which mathematically define the HEL through a general, three-dimensional strain-rate dependent constitutive law. We attempt here, through numerical simulations, to relate the amplitude and features of the HEL to a general constitutive equation for strain-rate dependent plastic behavior in metals, and to define the HEL mathematically for general forms of rate-dependent constitutive models.

ANALYSIS

The stresses and strains are decomposed in hydrostatic and deviatoric components. The hydrostatic components are related through the bulk modulus, K

$$S_{kk} = 3K e_{kk} \tag{6}$$

where repeated index means summation. The deviatoric components, S_{ij} and e_{ij} under elastic deformations, are related through the shear modulus, G

$$S_{ij} = 2G(e_{ij} - \tfrac{1}{3}e_{kk}\delta_{ij}) \tag{7}$$

where δ_{ij} is the Kronecker delta function. When plastic flow occurs, the S_{ij} and e_{ij} are related through the use of the Bodner–Partom (B–P) constitutive law. The equations are then incorporated into the one-dimensional STEALTH[11] finite difference computer code for numerical computations.

BODNER–PARTOM FLOW LAW

The B–P plastic flow equation is a state-variable based viscoplastic flow law. The governing equation was developed based on dislocation dynamics concepts and dynamic analysis[1, 12, 13]. It follows, in general, the state-variable based "unified" theories which decompose total strains or strain rates into elastic and inelastic components, thus

$$\dot{\varepsilon}_{ij} = \dot{\varepsilon}^{e}_{ij} + \dot{\varepsilon}^{p}_{ij} \tag{8}$$

where superscripts e and p refer to elastic and plastic, respectively, and dots denote derivatives with respect to time. This decomposition inherently assumes strains to be small. The elastic strain rates are related to the stress rates through Hooke's law

$$\dot{\varepsilon}^{e}_{ij} = \frac{1}{2G}\dot{\sigma}_{ij} + \frac{\dot{\sigma}_{kk}}{9K}\delta_{ij}. \tag{9}$$

This decomposition of strain into elastic and inelastic components provides for non-zero plastic flow at all times. There is no specific yield criterion associated with this formulation, rather yield occurs when plastic strains are no longer numerically small.

The flow law in the B–P equations takes the form

$$\dot{\varepsilon}^{p}_{ij} = D_0 \exp\left[-\left(\frac{n+1}{2n}\right)\left(\frac{Z^2}{3J_2}\right)^{n}\right]\frac{S_{ij}}{\sqrt{J_2}}. \tag{10}$$

This formulation assumes that plastic flow is in the direction of the applied stress and that the material hardens isotropically. In eqn (10), J_2 is the second invariant of the stress deviator, D_0 and n are constants, and Z is a state variable which is a measure of the material's "hardness" or resistance to plastic deformation. D_0 has the physical significance of being a limiting strain rate in shear while n is a measure of the strain-rate sensitivity of the material: smaller values of n produce higher rate sensitivity. It can be seen from eqn (10) that the plastic strain rates are always non-zero. However, from a numerical point of view, a certain value of J_2/Z is required before plastic strain rates become significant. Thus, the equivalence of a yield criterion in conventional plasticity is approached based on values of J_2 and Z.

The state variable Z is determined from an evolution equation

$$Z = Z_1 - (Z_1 - Z_0)\exp(-mW_p) \tag{11}$$

where Z_0, Z_1 and m are material constants and W_p is the plastic work

$$W_p = \int_0^t S_{ij}\dot{e}^{p}_{ij}\,dt \tag{12}$$

where Z_0 and Z_1 represent the initial hardness ($W_p = 0$) and maximum or saturation hardness, respectively, while m is a measure of the rate of strain hardening of the material. The evolution equation, eqn (11), can be written alternately in incremental form for computational purposes in a numerical procedure as

$$\dot{Z} = m(Z_1 - Z)\dot{W}_p \tag{13}$$

$$\dot{W}_p = S_{ij}\dot{e}^{p}_{ij}. \tag{14}$$

The formulation of these equations into a finite difference code requires few changes from numerical procedures which use a conventional yield criterion based on J_2 and an associated flow law. The calculations of S_{ij} requires an iterative scheme. Since the B–P model is a viscoplastic model, an algorithm in which the stress deviators are computed through a subincremental time stepping scheme was developed. The global time step, Δt, is further divided into small steps in a special purpose subroutine to describe the B–P model. At the end of each global time step, $\dot{e}_{ij}$, $\dot{e}$ and p are known; S_{ij}, σ_{ij} and $\dot{\varepsilon}^{p}_{ij}$ are unknown.

In the current numerical scheme, the plastic strain rates are estimated for each subincremental time step using eqns (10) and (11) with the value for J_2 calculated from the

Table 1.

	Z_0 (kbar)	Z_1 (kbar)	m (kbar^{-1})	n	D_0 (s^{-1})
1008	55	70	1.5	0.4	10^8
7039	5.6	7.6	2.8	4.0	10^8

known S_{ij} values at the beginning of the step. The elastic strain rates, $\dot{\varepsilon}^e_{ij}$, are estimated from the estimated $\dot{\varepsilon}^p_{ij}$ and the known total strain rates, $\dot{\varepsilon}_{ij}$. The new estimates for S_{ij} can be made from the following relationship:

$$\dot{S}_{ij} = E_{il}\dot{\varepsilon}^e_{lj} + \dot{p}\delta_{ij} \tag{15}$$

where E_{il} are the elements of the elastic modulus matrix.

Using the new estimates for $\dot{S}_{ij}$, the improved values for the plastic strain rates at the end of the subincremental time step can be computed. This procedure is continued until the values of $\dot{S}_{ij}$ computed for the two successive iterations converge to the same values within the tolerance limits. In addition to the deviatoric stresses and strain which are normally computed, only one additional quantity, the scalar Z, has to be tracked. Further, eqn (14) has to be computed at each time step for use in eqn (13). The total formulation of the deviatoric stress–strain behavior thus reduces to the use of eqns (8)–(10), (13) and (14), all written in incremental form.

RESULTS AND DISCUSSION

Two experiments were simulated numerically using the STEALTH[11] computer code. Each involved the impact of a 3 mm thick flyer plate against a 20 mm thick target plate at an impact velocity of 300 m s^{-1}. In each case, the flyer and target materials were identical. The first case utilized a constitutive model from data on 7039 aluminum, a material which is essentially strain rate independent[14]. The second case utilized constants for C1008 steel[14], a material which exhibits a high degree of strain rate dependence. The materials will be referred to as 7039 and 1008 henceforth for convenience. The numerical values of the constants for these materials were obtained through an iterative scheme which involved matching high strain rate Hopkinson bar data and steady state values of the HEL from thick target plate impact experiments. In the process, the plate impact experiment had to be numerically simulated on the computer and constants had to be varied to match the experimental free-surface velocity profile. No attention was paid to the transient wave propagation characteristics through the plate. The material constants for 1008 and 7039 are given in Table 1.

Having the material constants in hand, we now simulate the plate impact experiments for the two materials to study the details of the transient wave phenomena. A series of plots of stress vs time at different locations in the target plate are presented in Fig. 3 for 7039 and in Fig. 4 for 1008. The locations which the stress–time profiles correspond to are $x = 1$, 5, 10 and 15 mm from the impact face ($x = 0$) in the 20 mm thick target plate. Look, in particular, at the profile at $x = 5$ in Fig. 3 for 7039. Zero time is defined as the time of impact. The first wave does not arrive until nearly 0.7 μs. The stress rises rapidly to approximately 9 kbar (indicated by the arrow in Fig. 3), levels off very slightly, and then continues to rise from the slower plastic wave to a value of nearly 24 kbar at approximately 1 μs. At 1.6 μs, the wave begins unloading due to the release from the thin flyer. Compare these results with the schematic of Fig. 1. The same features are present, but they are less distinct in the actual profile.

Several features are apparent from these figures. First, until the stress wave has travelled approximately 5 mm, it is virtually impossible to discern the HEL from stress–time profiles in either of these materials. Second, the HEL becomes more distinct as the distance from the impact face increases. In both figures, the clearest definition of the HEL would appear to come from the profile obtained at $x = 15$ mm. Third, the amplitude of the HEL decreases

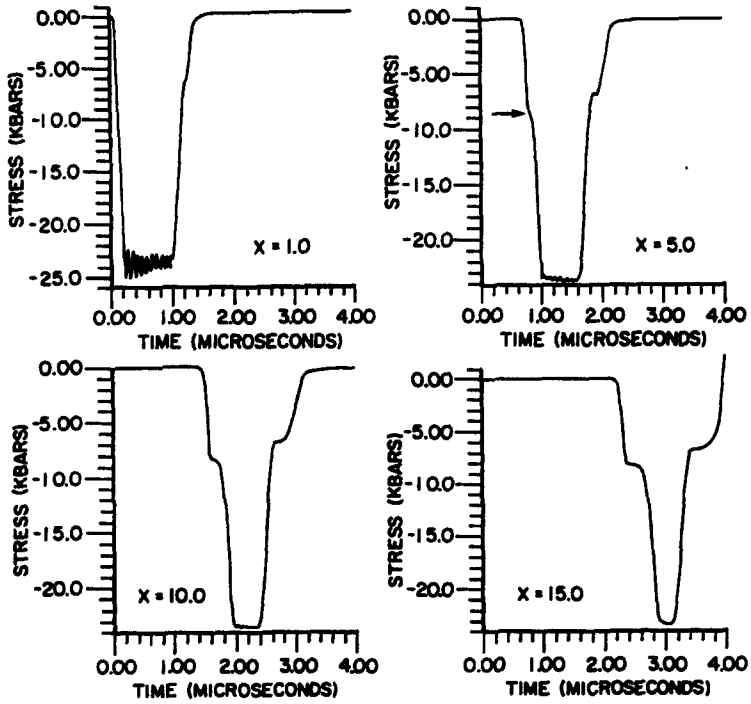

Fig. 3. Calculated stress–time profiles in 7039 aluminum (x in mm).

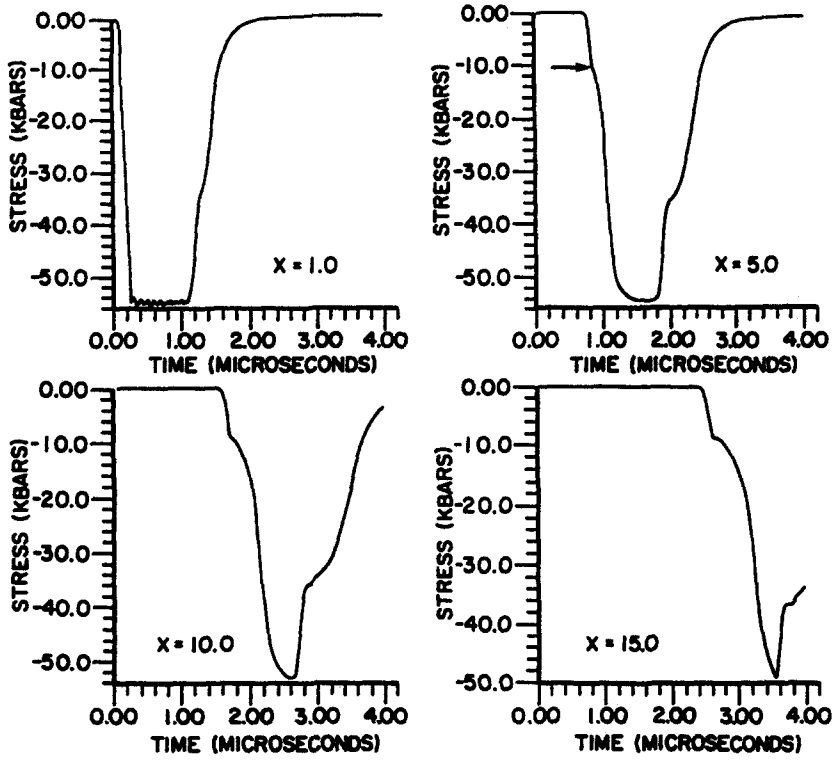

Fig. 4. Calculated stress–time profiles in C1008 steel (x in mm).

slightly with distance in 1008, a rate-dependent material. These values are subsequently plotted and compared with an analytical definition of the HEL.

A MATHEMATICAL DEFINITION OF HEL

Since these impact events are simulated on the computer, complete information is available about stresses and strains at all locations and for all times. Stresses that can be

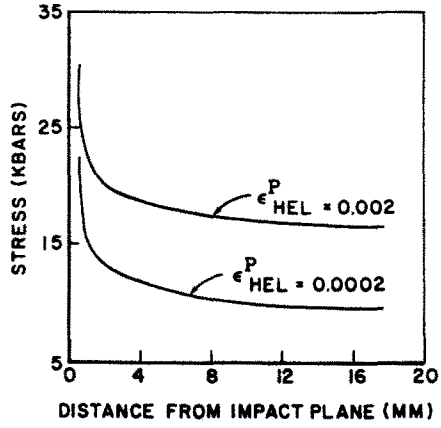

Fig. 5. Calculated HEL stress using plastic strain offset criteria.

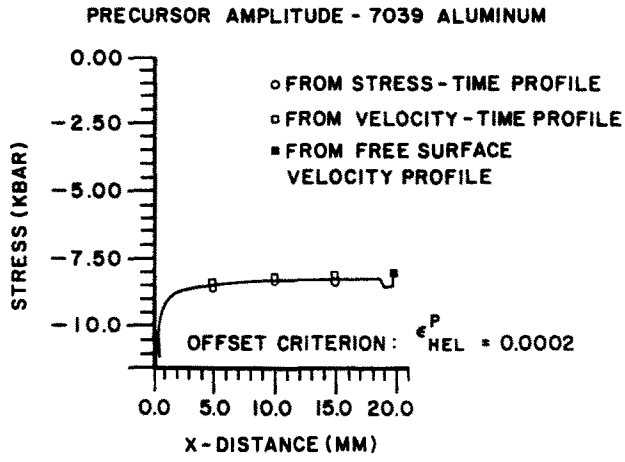

Fig. 6. Calculated precursor amplitude in 7039 aluminum (solid line represents 0.0002 offset criterion).

looked at include the normal stress, the stress deviator (effective stress) or the hydrostatic stress. Strain information is available in terms of elastic or plastic components or their deviators. Strain rates are also available. Since there is no formal definition of the HEL for a general, strain-rate dependent material, such as the one we are representing here with the B–P model, a criterion was sought which would reproduce the results that one would obtain graphically from the stress–time or velocity–time plots. At first, we defined the HEL as the longitudinal stress when D^p_1 or $\dot{\varepsilon}^p_x$ is equal to a small number ($\sim 10^{-10}$). Several plate impact test simulations were made and the precursor decay was plotted for each case. The value for the small number was changed in each simulation. The results showed unrealistic precursor decay along the target away from the impact plane.

Later, using a concept similar to the 0.2% offset criterion that has been used to determine the yield stress in a uniaxial quasi-static tension test, a critical value of effective plastic strain was proposed. Under the uniaxial strain state, the plastic strain ε^p_x in the wave propagation direction is equal to the effective plastic strain. It was found that large changes in the HEL resulted when going from values of 0.002–0.0002 as the critical value for ε^p_x. Figure 5 compares the HEL for 1008 using these two criteria. Further reduction of the critical value to 0.0001 provided a very slight change in the calculated HEL. The value of 0.0002 was thus arbitrarily chosen as the critical value of ε^p_x. When this value of plastic strain occurs, the corresponding stress is defined as the HEL, i.e. the material is no longer elastic. To verify this definition, the HEL values determined from the stress–time plots of Figs 3 and 4 are plotted with the HEL values determined from the offset definition in Figs 6 and 7 for 7039 and 1008, respectively. Also shown in the figures are values for the HEL as determined from the rear surface velocity profile, using eqn (2), and from computer generated velocity–time profiles at intermediate values of x, using

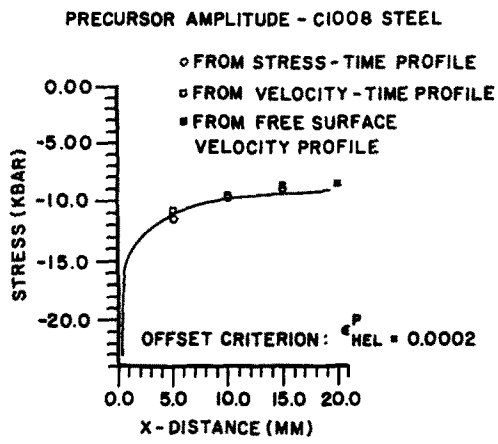

Fig. 7. Calculated precursor amplitude in C1008 steel (solid line represents 0.0002 offset criterion).

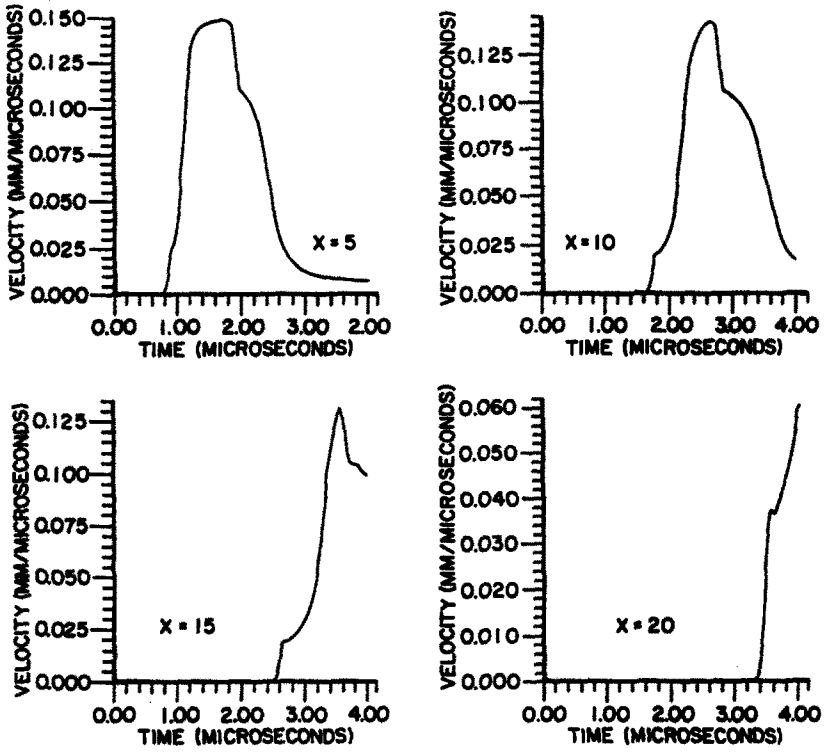

Fig. 8. Calculated velocity–time profiles in C1008 steel (x in mm).

$$\sigma_{\mathrm{HEL}} = \rho c v^* \tag{16}$$

where v^* is the velocity at the HEL. The values obtained from visually determined discontinuities in stress–time or velocity–time profiles are seen to agree well with the curve obtained using the mathematical definition of the HEL based on a 0.0002 plastic strain offset. The curve for 1008 steel is also representative of experimental precursor decay data on the same material obtained in an earlier investigation[15].

A series of plots of the velocity–time profile at different values of x is presented in Fig. 8 for 1008. Qualitatively similar results were obtained for 7039. The last plot is for $x = 20$ which corresponds to the free surface. Note that the velocity doubles compared to interior locations because the free surface generates a reflected wave travelling in the opposite direction. As in the case of the stress–time profiles, the HEL becomes more discernible with increase in propagation distance from the impact plane. This is due to the fact that the plastic wave propagates slower than the elastic precursor and thus the two waves tend to separate with increase in propagation distance. Again, the HEL cannot be distinguished until approximately 5 mm from the impact plane.

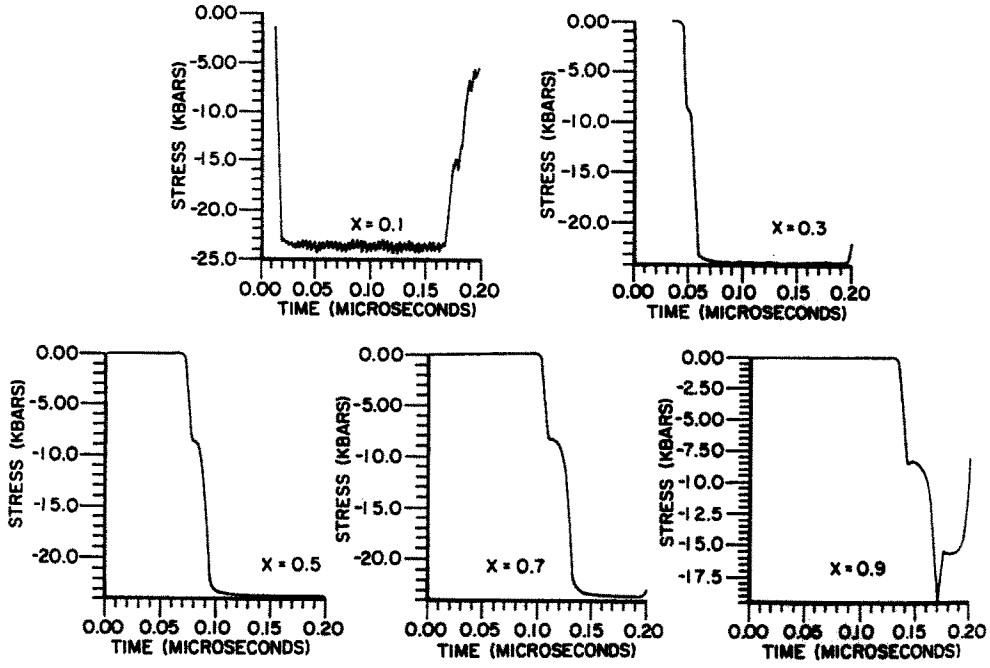

Fig. 9. Calculated stress–time profiles for thin plate impact simulation in 7039 aluminum.

An examination of Figs 6 and 7 shows that the HEL tends to assume higher values very close to the impact face. Since the material model used in this study exhibits strain-rate dependent behavior and the boundary condition at the impact surface consists of an instantaneous rise in velocity, it is not surprising to see high values of HEL near the surface. The values are not accurate because they result from a numerical calculation using discrete zones in the finite difference code and, furthermore, an artificial viscosity to smooth shock discontinuity[16]. To study the HEL close to the impact face, a second problem was simulated on the computer. This consisted of impacting a 0.5 mm thick flyer against an identical target material of 1.0 mm thickness at a velocity of 300 m s^{-1}. Both the 7039 and 1008 materials were used in these calculations.

Results for the thin plate simulations are presented in Figs 9 and 10 for 7039 and 1008, respectively. Shown are the stress–time profiles obtained at $x = 0.1, 0.3, 0.5, 0.7$ and 0.9 mm. For both materials, it can be seen that the HEL cannot be distinguished at $x = 0.1$ but is barely discernible at $x = 0.3$. For larger values of x, the HEL becomes more apparent. Contrast this with the results of the 3 mm/20 mm simulation in Figs 3 and 4 where the HEL could not be distinguished until $x = 5$ mm. The difference between the two cases is the much smaller time scale for the thin plate impact and the greatly improved numerical resolution in that calculation. The total target thickness is broken up into a number of discrete zones. For the thin target case, the sizes of the zones are 1/20th of those for the 20 mm thick case. Until unloading waves catch up with the elastic precursor, the two cases are identical because the wave does not know anything about the material thickness ahead of it during its first transit across the plate. Thus, in the performance of a real experiment using either embedded stress gages or free-surface velocity measurements, the ability to determine the HEL depends not only on the target thickness or distance from the impact plane but also on the time resolution of the instrumentation.

The 0.0002 plastic strain offset was used to analytically predict the HEL for the thin plate impacts. The results of that prediction are shown for 7039 in Fig. 11. Shown also on the figure are the values obtained directly from the stress–time profiles in Fig. 9. It can be seen that the agreement between those values and the one obtained from the offset criterion is excellent. Note that for 7039, a rate-independent material, the HEL does not change, even for values as small as $x = 0.1$ mm. The rise very close to the impact face is due to numerical accuracy, zone size and artificial viscosity. Because of the step input velocity

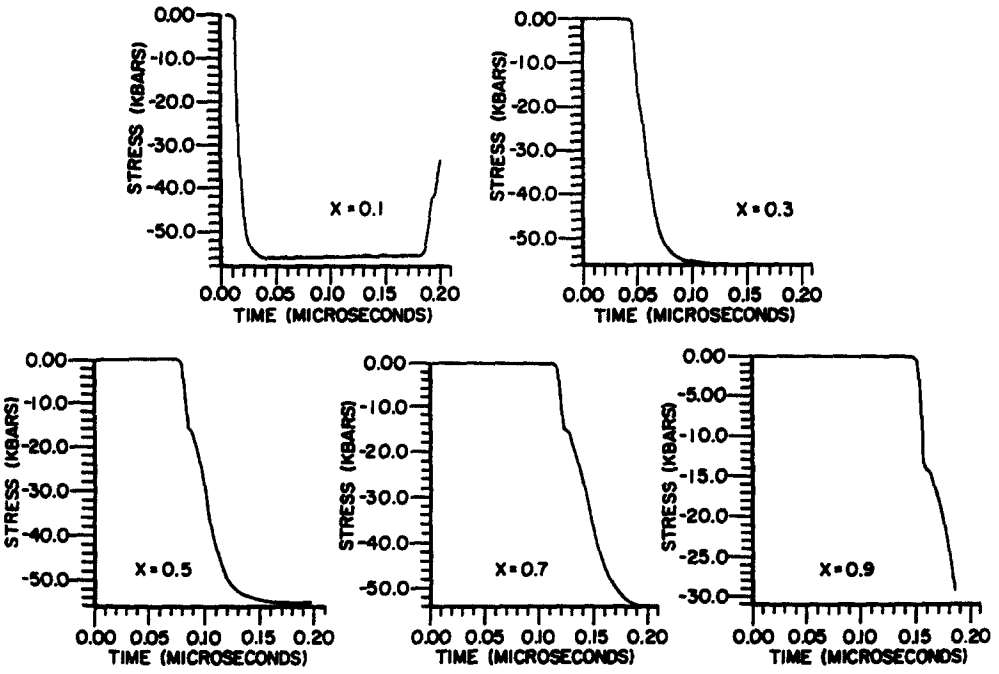

Fig. 10. Calculated stress–time profiles for thin plate impact simulation in C1008 steel.

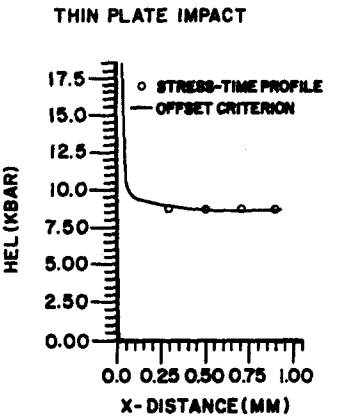

Fig. 11. Comparison of HEL from stress–time profiles and offset criterion in thin plate impact in 7039 aluminum.

boundary condition and the lack of instantaneous plastic flow in the strain-rate dependent constitutive law, the HEL cannot be defined immediately adjacent to the impact face. Compare the results in Fig. 11 with those of Fig. 6 for the thick flyer impact. In the latter case, the HEL appeared to rise below $x = 1$ mm. Again, this is an artifact of the numerical procedure.

For the strain-rate dependent 1008 material, the HEL values from the offset criterion (solid line) and from the stress–time plots of Fig. 10 (open circles) are presented in Fig. 12. Also shown are error bars associated with the determination of the HEL from the stress–time plots of Fig. 10. Note, again, the excellent correlation of HEL values determined by the two methods. As in the case of the thick plate impact as shown in Fig. 7, the results show an increased value for the HEL as the impact plane is approached. At distances within 1 mm of the impact face, the HEL takes on values in excess of 15 kbar. For large distances (see Fig. 7), the so-called "steady-state" value is approximately 9 kbar. Thus, the decay of the elastic precursor is evidence of the strain-rate dependence of plastic flow in a material.

To evaluate the effect of impact velocity on the offset definition of the HEL, two additional numerical simulations were conducted for the thick plate impact of 1008. In addition to 300 m s^{-1} which was the impact velocity used in the prior calculations, values

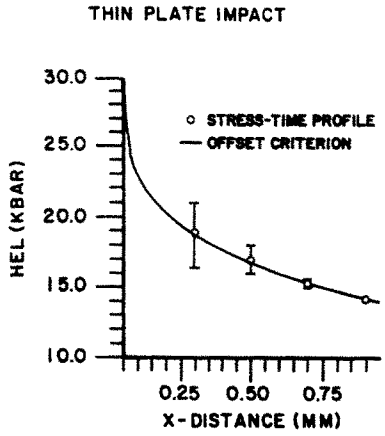

Fig. 12. Comparison of HEL from stress–time profiles and offset criterion in thin plate impact in C1008 steel.

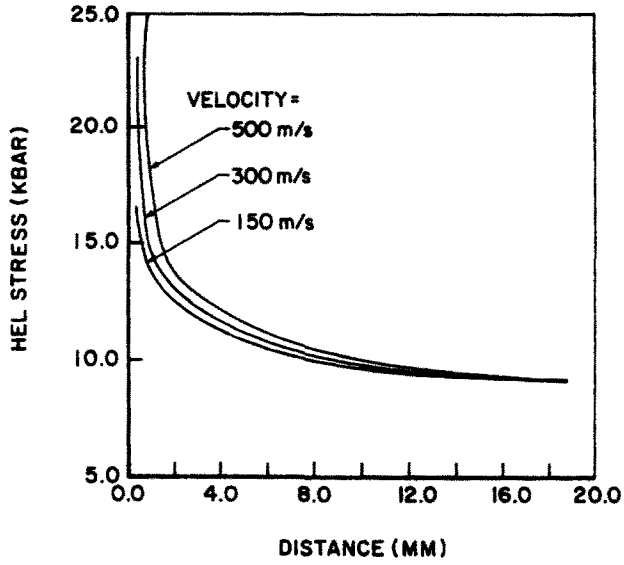

Fig. 13. Effect of impact velocity on calculated HEL in C1008 steel using 0.0002 offset criterion.

of 150 and 500 m s^{-1} were also employed. The results from the three cases are presented in Fig. 13. It can be seen that the HEL changes slightly with impact velocity as the impact plane is approached using a 0.0002 plastic strain offset criterion. Similar results were obtained for 7039. The differences, however, do not appear to be significant enough to warrant including a stress or pressure term in the criterion. The values of HEL along with the error bounds as determined from the stress–time profiles for these two other impact velocities are also summarized in Table 2. It can be seen that the stress–time profiles show essentially no difference in the value of the HEL as a function of impact velocity at a given value of x.

CONCLUSIONS

Analytical modeling of uniaxial strain waves generated from plate on plate impacts indicates that the decay of the elastic precursor amplitude (HEL) is a consequence of the strain-rate dependence of the materials. It has been shown that precursor decay can be predicted using a strain-rate dependent constitutive model whereas the amplitude of the precursor is constant for a strain-rate-independent model. Further, a formal mathematical definition of the HEL has been proposed. The HEL values obtained from stress–time or

Table 2. Values of σ_{HEL} from stress–time profiles

Material	Flyer/target (mm)	Impact velocity ($m\ s^{-1}$)	x-coordinate (mm)	σ_{HEL} (kbar)
Steel				
C1008	3/20	150	5	11.0±1.0
			10	9.4±0.2
			15	8.9±0.1
C1008	3/20	300	5	11.7±1.0
			10	9.6±0.5
			15	9.0±0.2
C1008	3/20	500	5	12.0±1.0
			10	10.0±1.0
			15	9.0±0.5
C1008	0.5/1.0	300	0.3	19.0±2.0
			0.5	17.0±1.0
			0.7	15.2±0.2
			0.9	14.1±0.1
Aluminum				
7039-T64	0.5/1.0	300	0.3	8.7±0.1
			0.5	8.7±0.1
			0.7	8.6±0.1
			0.9	8.6±0.1

velocity–time profiles agreed extremely well with the calculated values based on this definition. These values also correlated well with experimental data on the materials modeled in these numerical simulations.

The precursor decay was modeled using the viscoplastic flow law of Bodner and Partom (B–P) in a one-dimensional finite difference computer code. The B–P model used parameters obtained from a combination of high strain rate data from split Hopkinson bar tests and shock wave profiles in thick plate impact experiments. This approach differs from earlier approaches which were based on models calibrated primarily to fit experimental precursor decay data. The results here demonstrate that precursor decay can be predicted through a general, three-dimensional viscoplastic model, the parameters of which are determined independent of the precursor decay profile. Further, these constitutive models are not limited to any specific functional form.

REFERENCES

1. S. R. Bodner, Constitutive equations for dynamic material behavior. In *Mechanical Behavior of Materials Under Dynamic Loads* (Edited by U. S. Lindholm), pp. 176–190. Springer, New York (1968).
2. T. Nicholas, Material behavior at high strain rates. In *Impact Dynamics* (Edited by J. Zukas *et al.*), Chap. 8, pp. 277–332. Wiley-Interscience, New York (1982).
3. T. Nicholas, Elastic–plastic stress waves. In *Impact Dynamics* (Edited by J. Zukas *et al.*), Chap. 4, pp. 95–153. Wiley-Interscience, New York (1982).
4. Z. Rosenberg, D. Yaziv and Y. Partom, Calibration of foil-like Manganin gauges in planar shock wave experiments. *J. Appl. Phys.* **51**, 3702–3705 (1980).
5. L. M. Barker and R. A. Hollenback, Laser interferometer for measuring high velocities of any reflecting surface. *J. Appl. Phys.* **43**, 4669–4674 (1972).
6. G. E. Duvall, Propagation of plane shock waves in a stress-relaxing medium. In *Stress Waves in Inelastic Solids* (Edited by H. Kolsky and W. Prager), pp. 20–32. Springer, Berlin (1964).
7. A. H. Jones, C. J. Maiden, S. J. Green and H. Chin, Prediction of elastic–plastic wave profiles in aluminum 1060-0 under uniaxial strain loading. Symposium on the Mechanical Behavior of Materials under Dynamic Loads, Southwest Research Institute, San Antonio, Texas, September (1967).
8. A. M. Rajendran, A critical void growth failure criterion developed for dynamic and static loading conditions. Ph.D. Thesis, University of Washington, Seattle, Washington, December (1980).
9. R. P. Swift and I. M. Fyfe, Elastic/viscoplastic theory examined using radial cylindrical stress waves. *Trans. Am. Soc. Mech. Engrs*, Series E, *J. Appl. Mech.* **37**, 1134 (1970).
10. P. Perzyna, Fundamental problems in viscoplasticity. In *Advances in Applied Mechanics*, Vol. 9, pp. 243–377. Academic Press, New York (1966).
11. R. Hoffman, STEALTH, Lagrange explicit finite-difference code for solids, structural, thermohydraulic analysis, EPRI NP-2080, Electric Power Research Institute, Palo Alto, California, November (1981).
12. A. Merzer and S. R. Bodner, Analytical and computational representation of high rate of straining behavior. In *Mechanical Properties at High Rates of Strain* (Edited by J. Harding), Institute of Physics, Conference Series, No. 47, pp. 142–151. London (1979).
13. S. R. Bodner and Y. Partom, Constitutive equations for elastic–viscoplastic strain hardening materials. *ASME J. Appl. Mech.* **42**, 385–389 (1975).

14. A. M. Rajendran and S. J. Bless, High strain rate material behavior, AFWAL-TR-85-4009, Materials Laboratory, Wright-Patterson Air Force Base, Ohio, April (1985).
15. Z. Rosenberg and S. J. Bless, Stress wave measurements in impulsively loaded long steel rods with embedded Manganin gauges. *Proc. Int. Symp. on Intense Dynamic Loading and its Effects* (Edited by C. M. Chang and J. Ting), p. 742. Science Press, Beijing, China, June (1986).
16. M. L. Wilkins, Use of artificial viscosity in multi-dimensional fluid dynamic calculations. *J. Comput. Phys.* **36**, 281–303 (1980).